

## **Annex B6**

**Chapter in: A. T. Hubbard (Ed.)**

*Encyclopedia of Surface & Colloid Science"*, Marcel Dekker, New York, 2002 – in press.

### **HYDRODYNAMIC BEHAVIOUR AND STABILITY OF APPROACHING DEFORMABLE DROPS**

Theodor D. Gurkov, \* and Elka S. Basheva

Laboratory of Chemical Physics & Engineering, Faculty of Chemistry,  
University of Sofia, James Bourchier Avenue 1, Sofia 1164, Bulgaria

\*Author for correspondence (e-mail: tg@lcpe.uni-sofia.bg) on temporary leave from the Laboratory of Chemical Physics Engineering, Sofia.

#### **1. INTRODUCTION**

Liquid dispersions (emulsions and foams) are widespread in daily life and have multiple technological applications, so the problems connected with their formation and stability are considered to be of primary importance in colloid science. Much effort has been directed toward understanding what happens when two fluid particles (emulsion drops or gas bubbles) approach each other in a liquid medium. This determines to a large extent the initial stability of the dispersion, just after the phases are mixed together. At sufficiently small separations between the surfaces of the particles two effects come into play: (i) The presence of one particle influences the flow past the other one, giving rise to hydrodynamic interactions. The viscous friction in the liquid which is expelled from the intervening gap between the particles increases considerably, due to the geometric constraints; (ii) Direct intermolecular forces (such as e.g. van der Waals, electrostatic, steric, hydrophobic, hydration, etc.) become significant, so the surfaces are subjected to net attraction or repulsion. This usually happens at gap thicknesses below ~100 nm.

Drops and bubbles are deformable, and their shape is determined by the distribution of stresses applied locally along the interface. As the particles approach each other, the diminishing distance between the two liquid boundaries is associated with continuous changes in both the hydrodynamic and the direct interactions (for example, flattening of the front regions of the opposing surfaces brings about a sharp increase of the viscous resistance). Thus, further

deformation of the drops (bubbles) can occur, which in turn influences the various types of interactions.

Liquid dispersions are stabilised by adsorbed surface-active agents, whose role is manifold [1]: The liquid boundaries are immobilised, acquiring significant elasticity (and sometimes, surface viscosity), which damps the fluctuation capillary waves responsible for rupture of the interdroplet gap; the thinning of the latter gap is slowed down; the presence of surfactant gives rise to direct intermolecular repulsive interactions of different physical origin [2]. In order that these stabilising effects become operative, appreciable amount of surfactant should succeed to adsorb, which requires time. Especially in the first moments after the dispersion is formulated, it is very important how fast the fluid particles approach each other- this determines whether there will be enough time for surfactant adsorption before the interfaces touch each other and the drops coalesce. Moreover, the thinning rate itself is affected by the distribution of surfactant, which makes the overall picture rather complex.

In this article we discuss the velocity of approach of emulsion drops (or gas bubbles), focusing on the specific influence of the degree of tangential interfacial mobility (connected with the mechanisms of surfactant action), and the shape of the surfaces. The stability against growing corrugation waves is not considered here; neither do we enter into details about the intermolecular forces which ensure stability after the system reaches mechanical equilibrium at a constant gap thickness.

## 2. STAGES OF APPROACH OF FLUID PARTICLES IN A MEDIUM

Figure 1 provides an illustration of what happens when two deformable particles (drops or gas bubbles), suspended in a liquid, come to a close proximity under the action of an applied external force (e.g., buoyancy, or Brownian force) [3]. From a hydrodynamic point of view, the particles start “feeling” each other at distances much larger than their size. Then, however, the interactions are weak, and consequently, they can be calculated by means of series expansions with respect to the volume fraction, over the case of an unbounded fluid [4, 5]. Those hydrodynamic interactions are important for such properties of suspensions as the effective viscosity and the collective diffusion coefficient [5]. Below we will be interested in the limiting case of small separations, since it is relevant to the stability.

As the gap between the liquid boundaries (Fig. 1a) thins down, the viscous friction there increases and the corresponding stresses become comparable to the capillary pressure (the latter is responsible for keeping the drop interface curved). Therefore, the drops can undergo substantial deformation (if the pushing force is large enough). At a certain gap width (called inversion thickness,  $h_i$ ), the surface curvature in the film center (at  $r=0$ ) even changes its sign, and a concave lens-shaped region appears- Fig. 1b. This is called “dimple”, and has been a subject of numerous theoretical investigations (see e.g. Refs. [6, 7]). The inversion thickness is determined by the simple relation [8]

$$h_i = \frac{F}{2\pi\bar{\sigma}}, \text{ where } \bar{\sigma} = \frac{2\sigma_1\sigma_2}{\sigma_1 + \sigma_2}, \quad (1)$$

$F$  is the applied force on each particle (directed along the axis of symmetry,  $z$ ), and  $\sigma_1, \sigma_2$  are the interfacial tensions on the two boundaries  $S_1, S_2$  (Fig. 1). Danov et al. [9] have derived a transcendental equation for  $h_i$  including the potential energy of the surface forces. The dimple evolves quickly: after the initial growth it becomes hydrodynamically unstable and the liquid flows out to the meniscus region. An almost plane-parallel film is then formed- Fig. 1c.

The stage of dimple formation is possible when the driving force  $F$  is sufficiently large to overcome the energy barrier created by eventual electrostatic repulsion and by the increase of surface energy due to area dilatation during the deformation. It has been shown [9] that in the case of Brownian flocculation of small bubbles at low salt concentration dimple does not appear. Also, experimental studies of thin liquid films [10] have demonstrated that no dimple exists in films with very small diameter. Then, probably, the viscous resistance to thinning in the film center is too low to provide the high normal stresses required for dimpling.

Recent calculations for two approaching spherical emulsion drops in the presence of van der Waals attraction [11] have shown that dimple forms in the contact zone when the drops are large (with radius greater than  $\sim 80 \mu\text{m}$ ), whereas with small drops at a given gap width  $h_p$  the surfaces bend outwards (protrude toward each other), and two ‘‘pimples’’ are created. This phenomenon was discovered by Yiantsios & Davis [6] with pure liquid phases; Ref. [11] offers a full theoretical treatment, taking into account the surfactant diffusion, as well as the interfacial elasticity and viscosity. The pimple originates from the fact that the van der Waals disjoining pressure increases faster than the hydrodynamic pressure as the gap thickness  $h$  diminishes. At  $h < h_p$  the pimple spontaneously grows until the surfaces touch each other and the drops coalesce (i.e., instability occurs without fluctuations). The simple formula for  $h_p$ , derived in [11] for the case of tangentially immobile interfaces, reads

$$h_p = \sqrt{R_* A_H / (12F)}, \quad (2)$$

where  $R_*$  is the (mean) drop radius and  $A_H$  is the Hamaker constant of van der Waals interactions.

Once formed, the plane-parallel film between the drops (Fig. 1c) either thins further at a constant radius  $R$ , or remains in mechanical equilibrium at a relatively large thickness, of the order of 100-200 nm (if electrostatic repulsion is operative). Thermal fluctuations are responsible for continuous corrugation of the film surfaces by capillary waves- Fig. 1d. Van der Waals attraction amplifies these corrugations. When the derivative of the disjoining pressure,  $\partial\Pi/\partial h$ , is positive, the amplitude of the disturbances,  $\zeta$  (Fig. 1d), grows up spontaneously [12]. The hydrodynamic theory for film stability was developed in the works of many authors- see e.g. Refs. [12, 13, 14]. They define a critical thickness,  $h_{cr}$ , which is the average film thickness at the moment when the fluctuating surfaces just touch each other- this may result in either rupture of the film or appearance of black spots (Fig. 1e). Transitional thickness,  $h_t$ , is that at which the positive contribution to the

free energy, arising from the area increase because of the waves, and the negative contribution, due to the more intense van der Waals attraction in the thinner parts of the film, exactly compensate each other. At  $h > h_t$  the fluctuations are damped, and at  $h < h_t$  they grow. Besides,  $h_{cr} < h_t$ .

General expressions for  $h_{cr}$  and  $h_t$  have been obtained for plane-parallel films with tangentially immobile surfaces, by means of a long-wave stability analysis [12] (see also the reviews [5, 8, 15]). The case of slightly deformed spherical drops (in the presence of surfactant) is discussed comprehensively by Ivanov et al. [16]. The influence of different factors on  $h_{cr}$  was considered in Refs. [14, 15, 16]. For films  $h_{cr}$  was found to be about 20-50 nm [14], with no strong dependence on the film size. For very small drops  $h_{cr}$  can be as large as 200 nm, and with big drops it can fall below 10 nm [16]. With rising surfactant concentration  $h_{cr}$  first decreases slightly, and then reaches a plateau [14, 16]. A simple formula for estimation of  $h_{cr}$  in a plane-parallel film of radius  $R$  was proposed by Vrij (see e.g. Eq. (20) in Ref. [17]):

$$h_{cr} = 0.268 \left[ \frac{36\pi^3 A_H^2 R^4}{6.5 F \sigma} \right]^{1/7} \quad (3)$$

(it is valid for negligible  $\Pi$ ).

A stable thinner film in the spots (Fig. 1e) can form when there is a short-range (steric) repulsion between the adsorbed surfactant layers. The spots either expand in lateral direction or merge, and finally the whole film acquires a uniform thickness [15]. This film (usually called Newton Black Film, Fig. 1f) resembles a bilayer, as it may contain very little liquid in its interior. A characteristic feature here is the existence of a finite contact angle,  $\theta$ , which can be measured from the positions of the Newton fringes between the meniscus surfaces (readily visible by interference microscopy [8]). This angle depends on the integral of the surface forces, as demonstrated by the relation [18]:

$$\cos \theta = 1 + \frac{1}{2\sigma} \int_h^\infty \Pi(h) dh \quad (4)$$

(which holds for large film radii).

The hydrodynamic analysis of the thinning process in the gap between two fluid particles is usually carried out in the frames of the so-called lubrication approximation. It supposes quasi-steady flow (in the sense that the time derivative of the velocity in the Navier-Stokes equation is discarded, and time dependence may come only from the boundary conditions). Further, the Reynolds number is small ( $Re = \rho V h / \eta \ll 1$ , where  $\rho$  is the mass density,  $V$  is the thinning velocity, and  $\eta$  is the dynamic viscosity of the continuous phase). Hence, the inertia terms are neglected. The system usually has rotational symmetry (Fig. 1a). In addition,  $h \ll R$  (where  $R$  is a characteristic radial distance, e.g., film radius), and the radial component,  $v_r$ , of the fluid velocity  $\mathbf{v}$  is much larger than the vertical component,  $v_z$ . Under these circumstances, the governing equations of the flow read (cf. e.g. Ref. [19]):

$$\frac{\partial p}{\partial r} = \eta \frac{\partial^2 v_r}{\partial z^2} ; \quad \frac{\partial p}{\partial z} = 0 ; \quad \nabla \cdot \mathbf{v} = \frac{1}{r} \frac{\partial (r v_r)}{\partial r} + \frac{\partial v_z}{\partial z} = 0 . \quad (5)$$

Here  $p$  denotes pressure. When supplemented with suitable boundary conditions, these equations allow one to obtain a variety of useful solutions for particular cases. In general form the solution is presented in Ref. [5]. Some results for the velocity of film (gap) thinning will be reviewed below, with emphasis on the role of factors relevant to the stability of disperse systems.

### 3. INFLUENCE OF THE DEFORMATION ON THE RATE OF THINNING

When the droplets (bubbles) are very small, they remain spherical during their approach, up to the moment of direct contact of the interfaces (coalescence or flocculation). This is due to the fact that small particles have very high capillary pressure, so the hydrodynamic stresses are not large enough to cause deformation. Ivanov et al. [16] have demonstrated that for drops whose radius is below  $\sim 80 \mu\text{m}$  the inversion thickness  $h_i$  (at which significant deformation would take place) is smaller than 10 nm. Under such conditions the hydrodynamic interactions are irrelevant, because at  $h \sim 10$  nm the direct intermolecular forces will prevail overwhelmingly. In other words, those droplets will not be subject to deformation caused by the viscous friction in the gap. Danov & Ivanov [20] proved by numerical calculations that micrometer-size droplets maintain their spherical shape until coalescence. For such cases it is pertinent to apply the theory for approach of perfect spheres immersed in a liquid phase.

Deformation of real drops (or bubbles) can be caused not only by hydrodynamic stresses, but also by the direct molecular interactions. This problem has been analysed in details in Refs. [21, 22], and reviewed in [16]. The overall interaction energy is represented as a sum of van der Waals, electrostatic, ion-correlation, hydration, protrusion and steric, and oscillatory structural contributions, adding also the surface energy increase due to area expansion and the bending energy connected with the flattening of the interfaces in the central zone [16]. Minimum of the total energy of the two-particle system is sought, in order to determine the size of the (approximately) plane-parallel film between the deformed drops (a simple geometric model of truncated spheres is adopted).

In Table 1 (rows 1-3) we compare results for the velocity of thinning at different geometries of the intervening gap between particles with tangentially immobile interfaces. The Taylor velocity,  $V_{Ta}$ , refers to the case of two spheres (row 1); for a plane-parallel film one has the Reynolds velocity,  $V_{Re}$  (row 3). The more general configuration of two deformed spheres of different size with a (curved) film of constant thickness between them is considered in Ref. [9] (see row 2 in Table 1). Basically, at a given thickness and driving force, the viscous friction in a film is much higher than that in a gap between spheres (if  $h \ll R$ ). Therefore, drop deformation causes considerable slowdown of the mutual approach- the thinning velocity may be reduced by orders of

magnitude [5]. In the geometry of truncated spheres, it is interesting to estimate the relative importance of the film region and the gap between the spherical portions of the surfaces around the film (often called “meniscus”), for the overall resistance to thinning. This has been done by Kralchevsky et al. [5], who consider deformed drops with intervening uniform film (as in row 2 of Table 1). Appropriate dimensionless scale has been chosen, so that the obtained result is independent of film curvature. It turns out that the influence of the viscous friction in the zone encircling the film decreases the velocity of thinning (compared to  $V_{Re}$ ) about 3 times at larger distances,  $h \sim h_i$ , while for small distances,  $h \ll h_i$ , this influence vanishes ( $V \rightarrow V_{Re}$ ). The reason, of course, comes from the fact that when the gap is narrow the friction in the film becomes very high.

It is worthwhile to point out the strong dependence of  $V_{Re}$  on the film radius,  $R$  ( $V_{Re} \sim 1/R^4$ , cf. Table 1): large plane-parallel films will thin extremely slowly. Besides,  $h=0$  is reached for infinite time at any  $R$ , if the surfaces are immobile. The size of a film between two fluid particles (drops, bubbles) can easily be determined from the force balance on the deformed particle: in quasi-steady motion (absence of acceleration) the external force,  $F_{ext}$ , should be compensated by the capillary pressure. This gives the following relation [14]:

$$R^2 = F_{ext} R_* / 2\pi\sigma \quad (6)$$

(see Table 1 for the meaning of  $R_*$ ).

#### 4. INFLUENCE OF TANGENTIAL SURFACE MOBILITY ON THE RATE OF THINNING

The physical reason behind the dependence of the thinning velocity,  $V$ , on the degree of interfacial mobility is illustrated in Fig. 2. The velocity of lateral motion within the fluid/liquid surfaces,  $\mathbf{v}_s$ , serves as a boundary condition for the flow in the film. Thus, the overall outflux of liquid from the film to the meniscus (and therefore,  $V$ ) will be affected by  $\mathbf{v}_s$ . In the case of immobility,  $\mathbf{v}_s=0$  (Fig. 2a), the flux  $2\pi r \int_{-h/2}^{h/2} v_r(z) dz$  is small, while with fully mobile surfaces (Fig. 2b) it is large, and the thinning is therefore much faster. Complete mobility is realised when the system does not contain any surfactant.

In general, the balance of momentum transport at an arbitrary fluid interface  $S$  reads [23]

$$\nabla_s \cdot \mathbf{T}_s = \mathbf{n} \cdot (\mathbf{T}_2 - \mathbf{T}_1), \quad (7)$$

where  $\mathbf{n}$  represents the running unit normal to  $S$ ,  $\nabla_s$  is the surface gradient operator, and  $(\mathbf{T}_2 - \mathbf{T}_1)$  is the difference between the bulk stress tensors in the two adjacent phases, taken on  $S$ . The surface stress tensor,  $\mathbf{T}_s$ , incorporates the rheological properties of the interface, and usually obeys a constitutive relation of the form

$$\mathbf{T}_s = \sigma \mathbf{U}_s + \mathbf{T}_{s,visc} \quad (8)$$

Here  $\mathbf{U}_s$  is the surface unit tensor, and  $\mathbf{T}_{s,visc}$  accounts for the viscous stresses arising from the lateral motion of the molecules on  $S$ . In the absence of surfactants  $\mathbf{T}_{s,visc}$  vanishes, and the interfacial tension  $\sigma$  is constant. Therefore, from Eq. (7) it follows that  $\mathbf{n} \cdot (\mathbf{T}_2 - \mathbf{T}_1) = 0$  - the forces acting on the opposite sides of the liquid boundary should be equal.

In Table 1 (rows 4-6) we list some relations for  $V$ , taken from Refs. [5, 14, 24, 25, 26], valid for particles whose surfaces are fully mobile (i.e., without surfactant). Substituting typical values of the parameters, one can check that the thinning velocity  $V$  of a plane-parallel film in a system composed of pure fluid phases (row 6) is much greater than  $V_{Re}$ , in accordance with the expectations. The mobile fluid interfaces transmit the motion in the gap to the liquid inside the drops (cf. Fig. 2b). This leads to a complicated circulation of liquid within the drops, which contributes to the energy dissipation (note the presence of the viscosity of the disperse phase,  $\eta_d$ , in the equations for cases 5, 6 in Table 1). It is interesting to observe that the thinning velocity,  $V$ , of a film (row 6) should not depend on the viscosity of the continuous (film) phase,  $\eta$ . The latter prediction was confirmed experimentally [5].

Let us now consider the more important case when adsorbed surfactants are present. Then, the liquid boundaries acquire elastic and viscous properties, which render them partially (or fully) immobile. The dilatational and shear surface viscosities,  $\eta_{dil}$ ,  $\eta_{sh}$  [23, 27], account for the friction between the molecules on the interface when they are in lateral motion (the effects depend on the type of deformation of the two-dimensional continuum, hence two quantities are needed). The role of the surface viscosity ( $\eta_s \equiv \eta_{dil} + \eta_{sh}$ ) for the thin film hydrodynamics has been discussed in Ref. [8]. The conclusion is that at smaller film radius  $R$  and thickness  $h$  there is an increased influence of  $\eta_s$ , leading to interfacial immobilisation (manifested as a reduced value of  $V$ ).

The elasticity of the adsorbed surfactant layer has been shown to play a key role for the thinning rate and the film stability [3, 14]. Let us look at Fig. 2c, which depicts the flow pattern when the system contains a low-molecular-weight amphiphilic substance and the interfaces are partially mobile. Due to the outflow of liquid from the film to the meniscus during the thinning, a finite surface velocity,  $\mathbf{v}_s$ , exists. The moving interface carries away the surfactant molecules, so the adsorbed amount per unit area,  $\Gamma$ , diminishes in the central zone of the film. Since the interfacial tension  $\sigma$  is directly related to  $\Gamma$ , a lateral gradient of  $\sigma$  appears (with  $\partial\sigma/\partial r < 0$ ). The phenomenon is usually called ‘‘Marangoni effect’’ [23]. One writes  $\nabla_s \sigma = (-E_G / \Gamma) \nabla_s \Gamma$ , where  $E_G \equiv -d\sigma/d(\log \Gamma)$  is the Gibbs elasticity. Thus,  $E_G$  enters the stress balance equation (7). As a consequence of the above effect, the surface pressure (defined as  $\sigma_0 - \sigma$ , where  $\sigma_0$  refers to the bare liquid/fluid interface) is higher in the region close to the meniscus. This gradient of the surface pressure hampers the interfacial convection and substantially decreases the tangential mobility.

The situation is however complicated, due to the presence of additional routes of surfactant transport, which may offset (to some extent, or completely) the gradients of  $\sigma$ . First, there is surface diffusion, driven by the non-uniform distribution of surfactant: the corresponding flux is  $\mathbf{j}_s = -D_s \nabla_s \Gamma$  (with  $D_s$  being the surface diffusivity)- see Fig. 2c. Moreover, molecules can come from the bulk through diffusion, and adsorb to areas where  $\Gamma$  is lower than the equilibrium adsorption. All those effects, and their influence on the hydrodynamics of thinning, have been described in a comprehensive manner by Ivanov [14], and later reviewed in [3, 5, 8, 15, 16, 27]. The full mass balance of the species on the interface reads [3, 8]:

$$\frac{\partial \Gamma}{\partial t} + \nabla_s \cdot (\Gamma \mathbf{v}_s - D_s \nabla_s \Gamma) = \mathbf{j}_b \cdot \mathbf{n} , \quad (9)$$

where  $\mathbf{j}_b$  is the flux of molecules from the bulk. It may be either the continuous (film) phase or the drop phase (or both) which contain the surfactant, depending on its solubility.

In Table 1, rows 7-10, we quote some important results for the thinning velocity  $V$  in systems with surfactant. For foam films (row 8) the influences of the surface and bulk diffusion are accounted for by the terms with  $h_s$  and  $b$ , respectively. It is obvious that when the mass transport by diffusion (characterised by  $D_s$  and  $D$ ) is more pronounced  $V$  is greater- the interfaces are more mobile, as the continuous fluxes tend to restore the uniformity of the adsorption monolayers and the gradients of  $\sigma$  are damped. In thin films (at small  $h$ ) the effect of the surface diffusion dominates over that of the bulk diffusion. On the other hand, the elasticity suppresses the interfacial mobility: rising  $E_G$  causes  $V$  to diminish (row 8, Table 1). In the limit of high values of  $E_G$  the surface is immobilised completely, and  $V \rightarrow V_{Re}$ .

Comparison between the rows 8 and 9 in Table 1 reveals that no difference between the cases of foam and emulsion films exists when the surfactant is dissolved in the continuous phase. (The ‘‘foam parameter’’,  $\varepsilon_f$ , is usually much greater than the ‘‘emulsion parameter’’,  $\varepsilon_e$  [14].) Therefore, the presence of surfactant in the film practically extinguishes the effect of the energy dissipation in the drops.

Full tangential immobilisation of the interfaces can be achieved by increasing the surfactant concentration in the film up to values close to or above the CMC (the critical micellar concentration) [15]. Then  $E_G$ , and eventually  $\eta_s$ , become large enough. A numerical estimate of  $V/V_{Re}$  can easily be made according to the equation in row 8 of Table 1. We can use typical values of the relevant parameters, taking data from Table 2 in Ref. [8]. Thus,  $\eta = 0.01$  g/(cm.s) for water,  $D = 4 \times 10^{-6}$  cm<sup>2</sup>/s and  $E_G \partial \Gamma / \partial c = -\Gamma \partial \sigma / \partial c = 2 \times 10^{-10}$  mol/cm<sup>2</sup>  $\times$   $5 \times 10^8$  dyn.cm<sup>2</sup>/mol for ionic or non-ionic amphiphiles. The surface diffusion coefficient,  $D_s$ , is more difficult to assess; methods for its experimental measurement have been described by Russel et al. [28]. As an example, we can accept the result quoted in Ref. [15],  $D_s = 7 \times 10^{-5}$  cm<sup>2</sup>/s. Then, with Gibbs elasticity of about 5 dyn/cm near the CMC [8], one obtains  $V/V_{Re} = 1 + 1.2 \times 10^{-6} + 8.4 \times 10^{-7}$  cm/ $h$ . In other words, the

interfaces of films thicker than, say, 100 nm are immobile. The case of slightly deformed spherical emulsion drops has been discussed by Danov et al. [29, 11], who demonstrate that with different types of surfactant in the continuous phase appreciable mobility of the oil/water boundaries can be anticipated only at concentrations lower than  $\sim 0.01 \times \text{CMC}$ .

When surfactant is dissolved in the drop phase (row 10, Table 1), it cannot stabilise the system- the thinning rate is the same as in the case of pure liquid phases without any surfactant (row 6). The explanation of this important phenomenon is connected with the powerful diffusion transfer from the bulk of the dispersed phase toward the interface. From the side of the drops the surfactant diffusion is very fast and all gradients of  $\sigma$  are removed, so the liquid boundaries become completely mobile [5, 16]. (In contrast, enough surfactant cannot be supplied from the side of the thin and broad film which is in the process of further thinning.) The above effect serves as a basis for the process of chemical demulsification [5, 27]. One way to destroy an emulsion is to add surfactant which is soluble in the drops. It should possess sufficient surface activity (providing a significant decrease of  $\sigma$  upon adsorption). Then, the molecules of the demulsifier will quickly reduce the interfacial tension gradients, and the thinning rate will increase strongly (as if there were no surfactant at all)- the system will be destabilised and the approaching drops will coalesce.

When the interdroplet gap becomes sufficiently thin ( $h \sim 100$  nm or less), direct molecular interactions come into play. This may influence the driving force which pushes the particles against each other (it is denoted by  $F$  in Table 1). If the disjoining pressure ( $\Pi$ ) is not negligible,  $F$  will be equal to the applied external force,  $F_{\text{ext}}$ , minus the contribution of the interactions [16, 27]. For a plane-parallel circular film of radius  $R$  it can easily be shown that  $F = F_{\text{ext}} - \Pi(h)\pi R^2 = [P_c - \Pi(h)]\pi R^2$ , where  $P_c$  is the capillary pressure [14, 27]. Clearly, when  $\Pi$  is comparable to  $P_c$  the rate of thinning will be affected. In particular, if  $\Pi = P_c$  the film will rest in mechanical equilibrium- the thinning will stop altogether, owing to the absence of driving force. On the other hand, Nemeth et al. [30] have shown that van der Waals attraction ( $\Pi < 0$ ) accelerates the thinning.

In many cases the stability of fluid dispersions can be understood in terms of an interplay of hydrodynamic effects and direct molecular interactions. Explanation of the so-called ‘‘Bancroft rule’’ for obtaining a stable emulsion has been put forward in Refs. [5, 27, 31, 32]. This rule (in its most popular formulation) states that in order to produce a stable dispersion one must dissolve the amphiphile in the continuous liquid phase. It is believed that when water (w), oil (o), and surfactant are mixed together by vigorous mechanical agitation, both o/w and w/o dispersions form simultaneously [33]. It then matters which one of these two types of emulsions will survive in the first moments after the homogenisation. Definite answer to this question can be given when the surfactant is soluble in one of the phases only. If it is present in the continuous liquid (let us call this ‘‘System I’’), the thinning will be impeded by effects connected with partial interfacial immobility (due to Gibbs elasticity, etc.- see above). The decreased rate of thinning, in its turn, may lead to easier development of saturated adsorption monolayers with even higher elasticity and viscosity,

which repel each other ( $\Pi > 0$ ). On the contrary, in the reverse system with the same chemical composition (i.e., when the surfactant is in the drop phase, let's call this "System II"), the thinning will be very fast (if strongly repulsive  $\Pi$  does not prevent it), and coalescence will take place.

The thinning velocities in the two systems,  $V_I$ ,  $V_{II}$ , correspond to rows 9 and 10 of Table 1, respectively (if a plane-parallel film exists between the drops and the main viscous dissipation takes place there). As far as  $\varepsilon_f$  is usually of the order of 0.1, and  $\varepsilon_e \sim 10^{-2}-10^{-3}$  [16, 27], we get  $V_{II}/V_I \approx \varepsilon_f/\varepsilon_e \approx 10-100$ . Thus, the location of the surfactant has a dramatic effect on the film and drop stability: the mere phase inversion of the emulsion can change the lifetime by orders of magnitude. Experimental confirmations of this conclusion are available in the literature- see Refs. [34, 35].

It should be kept in mind, however, that the molecular interactions between the surfaces can be equally important as the hydrodynamics. The authors of Refs. [5, 32] derived an equation for  $V_{II}/V_I$  in films including the influence of  $\Pi$ :  $V_{II}/V_I \sim \frac{(P_c - \Pi_{II})^{2/3}}{(P_c - \Pi_I)}$ . When  $P_c$  is comparable to  $\Pi_I$  or  $\Pi_{II}$ , the effect of the hydrodynamics will be overridden and the respective emulsion becomes thermodynamically stable regardless of the extent of surface mobility. Discussion of the Bancroft rule in the case of slightly deformed spherical drops can be found in Ref. [16].

Complications arise when the surfactant is soluble in both bulk phases of an emulsion system. If its initial distribution between oil and water is non-equilibrium, then gradual redistribution will occur, which may lead to change of the stability with time. Yet another type of peculiar effects connected with the surfactant location are due to the mass transfer across the film interfaces- two phenomena which provide hydrodynamic stabilisation caused by continuous liquid fluxes are discussed in Section 6 below.

## 5. SIZE DEPENDENCE OF DROP STABILITY

Here we consider an example which illustrates how the inferences from the above theoretical considerations are confirmed by experiments in a real system. One can measure the lifetime,  $\tau$ , of oil drops pressed by buoyancy against a large flat oil/water interface: it turns out that the functional dependence of  $\tau$  vs. the drop radius can be quite different for small and for large drops [16, 36]. This is explained by the existing theory for the thinning velocity. When the system contains sufficiently *low* concentration of surfactant in the continuous (aqueous) phase, the hydrodynamics of the gap thinning will be the predominant factor which determines the stability. The drops coalesce with the homophase immediately after they arrive at a certain critical distance from it,  $h_{cr}$ , since equilibrium gap thickness cannot be reached. Ivanov & Kralchevsky [27] have put forward the prediction that the lifetime of such drops should exhibit a minimum when plotted as a function of the radius. The reason has been attributed to drop deformability- the thinning rate

essentially depends on the presence or absence of intervening film, whose formation is closely related to the drop diameter.

After having been released (e.g., from a capillary tip) in the volume of the continuous phase, an emulsion drop initially moves fast, according to the Stokes law, until it approaches the interface to a sufficiently small distance, so that the presence of the large surface be significant from the point of view of the hydrodynamics. Then, the drop markedly decelerates, which is of course due to the increased viscous friction in the gap. This sharp change in the law of drop motion can be observed directly [36]. We define the "lifetime",  $\tau$ , to be the time elapsed from the moment when the drop arrives at the interface and starts moving more slowly, until it disappears (by coalescing with the large homophase). Let us say that the thinning begins at some initial gap width,  $h_{in}$ , and ends at the critical thickness,  $h_{cr}$ :

$$\tau = \int_{h_{cr}}^{h_{in}} \frac{dh}{V(h)} . \quad (10)$$

Here, as usual,  $V(h)$  is the velocity of thinning at the current gap width  $h$ . In our further considerations we shall suppose that the interfaces are tangentially immobile. Such was really the case in the systems examined experimentally in Ref. [36] (some of them contained globular protein). Basheva et al. [36] measured  $\tau$  and compared the results with theoretical estimates based on particular expressions for  $V(h)$ .

Relatively large drops (with radius  $R_d \geq \sim 100 \mu\text{m}$  [36]) are deformed and a more or less plane-parallel intervening film exists- see the inset in Fig. 3. Then, the lifetime is almost entirely determined by the drainage of that film. One can use the formula for the Reynolds velocity of thinning (row 3 of Table 1), with  $F$  being the buoyancy force,  $F = (4\pi/3)\Delta\rho g R_d^3$ , where  $\Delta\rho$  is the density difference, and  $g$  is the gravity acceleration. The film radius,  $R$ , is determined from Eq. (6) (it can also be measured directly, by means of interference microscopy [36]). If one accepts Eq. (3) for the critical thickness of rupture, and assumes that  $h_{in} \gg h_{cr}$ , the following equation for  $\tau$  will result [36]:

$$\tau = 4.088\eta\sigma^{-8/7} A_H^{-4/7} (\Delta\rho g)^{5/7} R_d^{25/7} . \quad (11)$$

It predicts that the lifetime,  $\tau$ , should increase with the drop radius,  $R_d$ . Since  $F$  also rises, as  $F \sim R_d^3$ , we come to the conclusion that the higher the pushing force, the longer the drops live. This inference seems paradoxical at a first sight, but the explanation is simple: larger force creates larger drop deformation (Eq. (6)), and the thinning velocity depends strongly on the film radius ( $V \sim 1/R^4$  - Table 1). The effect of the increased viscous friction in a wider film outweighs the fact that bigger  $F$  favours faster drainage if all other parameters are fixed.

Small droplets (with  $R_d < \sim 100 \mu\text{m}$ ) maintain their spherical shape up to the moment of coalescence [36]. In the latter case we can use the Taylor formula for a hard sphere which

approaches a solid plane wall (cf. row 1 in Table 1, with  $R_2 \rightarrow \infty$ ). Then, for gravity-driven settling, Eq. (10) yields:

$$\tau = \frac{9\eta}{2\Delta\rho g} \frac{1}{R_d} \log \left[ \frac{h_{in}^{(Ta)}}{h_{cr}} \right], \quad (12)$$

where  $h_{in}^{(Ta)}$  denotes the gap thickness at which the drop motion switches from Stokes' to Taylor's regime. In principle,  $h_{in}^{(Ta)}$  and  $h_{cr}$  may depend on  $R_d$ . However, the dependence of the logarithm should be rather weak. Therefore, we may accept that  $\tau \sim 1/R_d$ . Equation (12) predicts that the lifetime,  $\tau$ , should diminish with the increase of the drop radius,  $R_d$  (and the driving force,  $F$ ). This trend is just the opposite to what follows from Eq. (11).

Experimental data for  $\tau$  vs.  $R_d$  [36] are plotted in Fig. 3. The solid lines are drawn according to Eq. (11),  $\tau = 45.7 R_d^{25/7}$  (the right-hand branch, Reynolds regime), and Eq. (12),  $\tau = 0.145/R_d$  (the left-hand branch, Taylor regime). Obviously, the qualitative agreement between the observed and predicted dependencies is good (more detailed discussion about the parameters can be found in Ref. [36]). The coalescence behaviour in the three regions (small, medium-size, and large drops) is following quite different trends, and this is due to the drop deformability which affects the hydrodynamics of gap thinning. A shallow and broad minimum exists, as expected, and in the interval of  $R_d \sim 20\text{-}500 \mu\text{m}$  the drops are very unstable. In fact, when  $R_d > \sim 100 \mu\text{m}$  films are formed, but this does not improve the drop stability significantly (up to  $R_d \sim 500 \mu\text{m}$ ). Actually, in this interval the extent of droplet deformation is small, so the effect associated with increased viscous resistance will not be very well pronounced. One more point to be noticed in Fig. 3 is the marked scattering of the measured values of  $\tau$  for a given  $R_d$ . The reason for this is discussed briefly in Section 7 below.

## 6. NON-EQUILIBRIUM EFFECTS DUE TO SURFACTANT REDISTRIBUTION IN THIN LIQUID FILMS

Now we comment on the behaviour of model systems of emulsion type (liquid films) when the surfactant is soluble in both phases but is initially dissolved in one of them only. Then, intense fluxes of amphiphilic molecules across the oil/water interfaces appear, and this mass transfer drives liquid convection. The exchange of liquid between the film and the Plateau border (the meniscus) strongly augments the stability. Such an effect can be quite beneficial in improving the stability of real emulsions just after their homogenisation. Two complementary model cases are possible:

(i) surfactant is initially dissolved in the film phase (water), and diffuses towards the surrounding oil, through the surfaces. In this system the fascinating phenomenon of spontaneously

oscillating dimple has been discovered [37]. The dimple is fed by Marangoni-driven convective influx of aqueous phase from the meniscus [38], and the film remains stable for a long time;

(ii) surfactant is dissolved in the ambient oil phases and diffuses towards the aqueous film. Osmotic stabilisation is then operative, due to quick formation of surfactant micelles in the film. The difference between the micellar concentrations in the film and in the meniscus induces continuous liquid circulation which keeps the film thick and stable [39, 40].

Films are often formed in a glass capillary, and observation is carried out in reflected monochromatic light (by interference microscopy) [37, 38, 39]. The used non-ionic surfactants, such as e.g. Tweens (fatty acid esters of oxyethylene-substituted sorbitan) are typical in that they are readily soluble both in water and in oil, and diffuse rapidly. Figure 4a illustrates the processes during one dimple cycle (case (i)). First, the dimple grows inside the film until reaching a certain size, then it rushes out, and a new dimple starts to grow again. Figure 4b presents an interference image of a film with a large dimple which just starts flowing out (the Newton fringes are visible). This cyclic process can go on for several hours, until the equilibrium distribution of surfactant is reached- then the formation of dimples ceases and the film eventually ruptures [37]. Of course, one has to distinguish this oscillating dimple from the dimple which occurs during film thinning (as described in Section 2 above)- the latter has nothing to do with non-equilibrium distribution of surfactant.

It is important to note that with pre-equilibrated phases there is no oscillatory dimpling at all. Moreover, the phenomenon can manifest itself even in the presence of relatively high amount of electrolyte (0.1 M NaCl). The films remain rather thick (up to ~300 nm). These findings confirm the decisive stabilising role of the hydrodynamic fluxes, since under such conditions no other sources of stabilisation can be operative.

The dimpling process is driven by exhausting of surfactant in the film interior and on the interfaces, due to retarded supply from the meniscus (the thickness of the film is much smaller than its diameter). The existing gradients of adsorption and interfacial tension bring about tangential motion of the surfaces (Marangoni effect), coupled with convective flux of surfactant solution into the film. Thus, liquid phase is sucked from the Plateau border, giving rise to high thickness and stability. The complete theory of the described phenomena, together with its experimental confirmation, can be found in Ref. [38].

In the opposite case (ii), when nonionic surfactant is initially dissolved in the oil phase and diffuses across the interfaces into the film, again high stability and large thickness (above 100 nm) is observed [39, 40]. A specific dynamic pattern then emerges: formation of channels of higher thickness, as a consequence of the intense hydrodynamic circulation of the film phase. Figure 4c shows a film with such a channel; the directions of the continuous inflow and outflow of aqueous phase are indicated by arrows. The non-equilibrium phenomena can last up to 24 hours. After the mass transfer ceases, and when preequilibrated phases are used, the films spontaneously thin down (within a few minutes) to very thin “black” films ( $h \approx 10$  nm), and rupture.

Qualitative explanation of the above processes has been proposed in Ref. [39]: The stabilisation of the thick aqueous film is due to the higher osmotic pressure of surfactant aggregates (micelles) in the film, compared to that in the surrounding Plateau border. Because of diffusion through the oil/water interfaces, the surfactant concentration in the aqueous film gradually increases. Micelles are formed quickly; the monomer concentration in the water remains constant, so the diffusion flux coming from the oil cannot stop until the equilibrium distribution is reached. Meanwhile, the thin and broad film gets enriched with surfactant micelles, while their concentration in the surrounding voluminous meniscus remains low (the micellar diffusion is slow and the diameter of the film is much larger than its thickness). The increased osmotic pressure of micelles in the film overcomes the capillary pressure and brings about an influx of liquid from the Plateau border. In this way the circulation shown in Fig. 4c is engendered.

## 7. STATISTICAL NATURE OF THE COALESCENCE PROCESS

Basically, one mechanism for coalescence of emulsion drops which are in a close contact includes spontaneous growth of fluctuation waves on the two opposing o/w interfaces until the latter touch each other- this leads to rupture of the interdroplet gap [13]. Such a picture would imply that the coalescence is a stochastic phenomenon- its occurrence is expected to depend on the probability for emergence of an appropriate fluctuation. The wave mechanism is relevant to relatively thick films, whereas in bilayers (Newton black films) the rupture usually happens because of formation and growth of holes [41, 42]. The importance of the curvature properties of the surfactant monolayer (the spontaneous curvature, bending and saddle-splay elastic moduli) for the hole nucleation has been emphasized by Kabalnov & Wennerstrom [41]. Here we will confine ourselves to a discussion of the coalescence caused by thermally excited fluctuation waves. For more details about the hole nucleation mechanism the reader is referred to the works [41, 42], and the literature cited therein.

The experiment confirms the conjecture for a statistical nature of the coalescence process. For example, the data in Fig. 5 demonstrate that oil drops released toward a large oil/water interface have lifetimes which are randomly scattered in a wide interval (from 0 to ~100 s, in a system containing protein). Then, it is impossible to take average value of the lifetime, as the error would be  $\pm 100\%$ . These data have to be analysed in a different way.

It is convenient to determine the number of drops,  $N(t)$ , which survive until the moment  $t$  (as done e.g. in Refs. [43, 44]). The quantity  $(-1/N)dN/dt$  will have the meaning of a probability for drop burst per unit time (one may realise that  $dN$  is the number of ruptures within the time interval  $dt$ ). For the sake of brevity, we will use the notation  $w \equiv (-1/N)dN/dt$ . In principle,  $w$  can be (and often is) time-dependent, due to different reasons: (i) the liquid film between the drops (the gap) may be gradually thinning; (ii) there may be a continuous adsorption of surfactant molecules onto the o/w interfaces; (iii) ageing of the surfaces may take place: especially with globular proteins

a two-dimensional entangled network can form, and the interface may acquire viscoelastic properties; etc. All those factors change the conditions for appearance and growth of fluctuations. Formally, one is permitted to write an expansion:

$$-\frac{1}{N} \frac{dN}{dt} \equiv w(t) = w_0 + 2w_1(t-t_0) + \dots, \text{ or } -\log \frac{N}{N_{\text{tot}}} = w_0(t-t_0) + w_1(t-t_0)^2 + \dots, \quad (13)$$

where  $w_0 = w(t=t_0)$ ,  $2w_1 = (\partial w / \partial t)_{t=t_0}$ , and  $t_0$  is the moment when coalescence is first observed in the system. We used Eq. (13) to plot the data from Fig. 5 in the appropriate scale ( $N_{\text{tot}} = 63$ ), and the result is represented by the curve (a) in Fig. 6. It is seen that the parabolic function (13) with two parameters,  $w_0$ ,  $w_1$ , provides an adequate description of the experimental dependence. It is worthwhile to mention that the points in Fig. 6a correspond to drops with different diameters. From Fig. 5 it is evident that in the chosen interval the lifetime does not depend on the drop size. Therefore, all data should indeed lie on the same smooth curve (Fig. 6a).

Similar measurements of  $N(t)$  have been carried out by other authors (see e.g. Ref. [44] and the review [43]). In our Fig. 6, case (b), we plot results from Ref. [44] for the stability of aqueous drops (with a fixed radius of 0.19 cm) pressed by buoyancy against a large paraffin/ water interface. The scale suggested by Eq. (13) again proves satisfactory in representing the data. What is more interesting here, however, is the fact that the system does not contain any surfactant, and yet the typical shape of the  $\log(N(t))$  curve remains unchanged. This leads us to the important conclusion for universality of the stochastic nature of the coalescence event. The underlying physics is easily understood in view of the presence of thermal corrugations on the two opposing interfaces.

As far as the surface fluctuations are in the form of waves which propagate in a liquid medium, we may stipulate that the energy of a given wave will be proportional to the square of its amplitude  $A$ :

$$\text{energy} \sim \text{amplitude}^2 \equiv A^2. \quad (14)$$

The probability,  $dP(A)$ , for appearance of a wave whose amplitude is in the infinitesimal interval from  $A$  to  $A+dA$  will be given by the Gibbs' distribution:

$$dP(A) = \frac{1}{Q} \exp(-CA^2) dA. \quad (15)$$

Here  $C$  is a constant which involves the thermal energy,  $kT$ , the wave frequency, the film size, etc., and  $Q$  is the partition function,  $Q = \int_0^\infty \exp(-CA^2) dA = [\sqrt{\pi/C}]/2$ . Now one can realise that if two drops are separated by a liquid film or gap of thickness  $h$ , rupture will occur when  $A$  exceeds  $h$ . The corresponding probability for emergence of a wave with amplitude larger than  $h$  will be

$$P(A \geq h) = \frac{1}{Q} \int_h^\infty e^{-CA^2} dA = \text{erfc}(h\sqrt{C}). \quad (16)$$

This is equal to the fraction of the fluctuations which are efficient in causing immediate drop coalescence; when multiplied by some characteristic frequency for excitation of corrugations it would give  $w$ , so we may write

$$-\frac{1}{N} \frac{dN}{dt} = w[h(t)] \sim \operatorname{erfc}(h\sqrt{C}) = \operatorname{erfc}(h_0\sqrt{C}) + 2\sqrt{\frac{C}{\pi}} e^{-Ch_0^2} (h_0 - h) + \dots \quad (17)$$

In Eq. (17) we made expansion for small changes of  $h$  with respect to the value  $h_0 = h(t = t_0)$ . It is now clear why  $w$  has to depend on the film thickness,  $h$ . As  $h$  decreases with the film thinning,  $w$  is expected to augment (i.e., rupture will happen more readily). What is actually observed in the experiment is that  $w$  gradually rises with time (cf. the slopes of the three curves in Fig. 6), even in a system without surfactant (case b). Bearing in mind the above qualitative considerations, we may attribute this effect to film thinning. (Continuous adsorption of surfactant, or strengthening of the adsorption monolayer due to ageing, if existent, would have led to the opposite trend of diminishing rupture probability  $w$  as a function of time.)

If, for example, a plane-parallel interdroplet film with radius  $R$  obeys the Reynolds law of thinning (which is pertinent to tangentially immobile surfaces), then the integration of  $-dh/dt = V_{Re}$  (Table 1) yields

$$\frac{4F}{3\pi\eta R^4} (t - t_0) = \frac{1}{h^2} - \frac{1}{h_0^2} \approx \frac{2}{h_0^3} (h_0 - h) . \quad (18)$$

Here it was supposed that  $h_0 - h \ll h_0$ . If  $F$  is due to buoyancy ( $F \approx 0.05$  dyn for a drop with radius 0.05 cm and density difference with water  $\approx 0.1$  g/cm<sup>3</sup>),  $\eta = 0.01$  g/(cm.s),  $R \approx 63$   $\mu$ m (according to Eq. (6)), then a film with  $h = 20$  nm will reach a thickness of  $\approx 16$  nm for a period of about 100 s. In other words, the thinning is relatively slow. Equation (18) suggests that in this regime  $h_0 - h$  is proportional to  $t - t_0$ , so Eq. (17) is compatible with the observed linear dependence of  $w$  upon time (integrated form of the latter is shown in Fig. 6- cf. Eqs. (13)). There are cases when the film eventually rests in mechanical equilibrium and retains a constant thickness, at least for a certain period of time. Then  $w$  will remain constant (see the curve (c) in Fig. 6).

One can easily determine the parameters  $w_0$  and  $w_1$  in the expansion (13) from fits of experimental data- numerical values are listed in the caption to Fig. 6. The probability  $w_0$  varies between 0.09 s<sup>-1</sup> and 0.01 s<sup>-1</sup> for the selected systems. Of course, the quantities  $w_0$ ,  $w_1$  will be quite sensitive to the film properties, as well as to such characteristics of the system composition as the surfactant type and concentration. Figure 6 presents only results for very dilute systems with proteins, in which the stability is not significantly different from the case without surfactant (some more data can be found in Ref. [36]). We wish to mention that when bigger amount of surfactant is present the coalescence stops altogether and the emulsion drops are completely stable. This

complies with the known ability of amphiphilic substances to suppress the interfacial corrugations [23, 33] (through increasing the surface elasticity and viscosity).

## CONCLUSIONS

Our discussion demonstrates that the stability of two fluid particles (drops or bubbles), which move toward each other in a liquid medium, is substantially influenced by the hydrodynamics of gap thinning. The velocity of approach depends on the extent of deformation of the liquid interfaces: flattening of the front zone and appearance of a film brings about a considerable increase of the viscous resistance to thinning. The role of surfactants is connected with the tangential mobility of the fluid boundaries- there is an interplay of interfacial elasticity, viscosity, surface and bulk diffusion of the amphiphilic species, which ultimately determine the rate of thinning. In this context, the surfactant location and its solubility turn out to be quite important. Non-equilibrium effects due to surfactant redistribution between the bulk phases can stabilise the emulsion systems, as a result of the engendered continuous liquid fluxes.

Sometimes the hydrodynamic regime of the liquid flow in the gap between the particles is the main relevant factor for stability. Then, a peculiar dependence of the drop lifetime,  $\tau$ , on the drop radius,  $R_d$ , is predicted and experimentally observed- the function  $\tau(R_d)$  passes through a minimum. The direct molecular interactions, on the other hand, may significantly affect the thinning, or even play a decisive role, overriding the hydrodynamic effects. Theoretical considerations make it possible to understand (and clarify the limitations of) empirically established rules for formulation of stable emulsions.

Experimental evidence for the statistical nature of the coalescence event is discussed. The probability for drop rupture increases with time, which may be attributed to film thinning- an explanation is proposed, based on the conditions for appearance of an effective fluctuation.

## ACKNOWLEDGEMENTS

The work in LCPE-Sofia was financially supported by INCO-Copernicus Project # IC15 CT98 0911 of the European Union. TG wishes to thank Krassimir D. Danov for the helpful discussions and provided literature.

## REFERENCES

- 1 Hunter, R.J. *Foundations of Colloid Science*; Clarendon Press: Oxford; Vol. 1, 1987; Vol. 2, 1989; *Introduction to Modern Colloid Science*; Oxford University Press: New York, 1993.
- 2 Israelachvili, J.N. *Intermolecular and Surface Forces*; Academic Press: London, 1992.
- 3 Ivanov, I.B.; Dimitrov, D.S. Thin film drainage. In *Thin Liquid Films: Fundamentals and Applications*; Ivanov, I.B., Ed.; Marcel Dekker: New York, 1988; Chapter 7, p. 379-496.
- 4 Happel, J.; Brenner, H. *Low Reynolds Number Hydrodynamics with Special Applications to Particulate Media*; Prentice Hall: Englewood Cliffs, New Jersey, 1965.
- 5 Kralchevsky, P.A.; Danov, K.D.; Denkov, N.D. Chemical physics of colloid systems and interfaces. In *Handbook of Surface and Colloid Chemistry*; Birdi, K.S., Ed.; CRC Press: Boca Raton, Florida, 1997; Chapter 11, p. 333-494.
- 6 Yiantsios, S.G.; Davis, R.H. *J. Colloid Interface Sci.* **1991**, *144*, 412.
- 7 Ascoli, E.P.; Dandy, D.S.; Leal, L.G. *J. Fluid Mech.* **1990**, *213*, 287.
- 8 Kralchevsky, P.A.; Danov, K.D.; Ivanov, I.B. Thin liquid film physics. In *Foams: Theory, Measurements and Applications*; Prud'homme, R.K., Ed.; Marcel Dekker: New York, 1995; Chapter 1, p. 1.
- 9 Danov, K.D.; Denkov, N.D.; Petsev, D.N.; Ivanov, I.B.; Borwankar, R.P. Coalescence Dynamics of Deformable Brownian Emulsion Droplets. *Langmuir* **1993**, *9*, 1731-1740.
- 10 Velev, O. D.; Constantinides, G. N.; Avraam, D. G.; Payatakes, A. C.; Borwankar, R. P. Investigation of thin liquid films of small diameters and high capillary pressures by a miniaturized cell. *J. Colloid Interface Sci.* **1995**, *175* (1), 68-76.
- 11 Valkovska, D.S.; Danov, K.D.; Ivanov, I.B. Surfactants role on the deformation of colliding small bubbles. *Colloids Surfaces A* **1999**, *156* (1-3), 547-566.
- 12 Ivanov, I.B.; Radoev, B.P.; Manev, E.; Scheludko, A. Theory of the critical thickness of rupture of thin liquid films. *Trans. Faraday Soc.* **1970**, *66* (part 5, N 569), 1262-1273.
- 13 Maldarelli, Ch.; Jain, R.K. The hydrodynamic stability of thin films. In *Thin Liquid Films: Fundamentals and Applications*; Ivanov, I.B., Ed.; Marcel Dekker: New York, 1988; Chapter 8, p. 497.
- 14 Ivanov, I.B. Effect of surface mobility on the dynamic behavior of thin liquid films. *Pure & Applied Chem.* **1980**, *52*, 1241-1262.
- 15 Danov, K.D.; Kralchevsky, P.A.; Ivanov, I.B. Equilibrium and dynamics of surfactant adsorption monolayers and thin liquid films. In *Handbook of Detergents*; Broze, G., Ed.; Marcel Dekker: New York, 1999; Chapter 9, p. 303-418.
- 16 Ivanov, I.B.; Danov, K.D.; Kralchevsky, P.A. Flocculation and coalescence of micron-size emulsion droplets. *Colloids Surfaces A* **1999**, *152*, 161-182.
- 17 Hartland, S. Coalescence in dense-packed dispersions. In *Thin Liquid Films: Fundamentals and Applications*; Ivanov, I.B., Ed.; Marcel Dekker: New York, 1988; Chapter 10, p. 663.

- 18 Ivanov, I.B.; Toshev, B.V. Thermodynamics of thin liquid films. II. Film thickness and its relation to the surface tension and the contact angle. *Colloid & Polymer Sci.* **1975**, 253 (7), 593-599.
- 19 Landau, L.D.; Lifshitz, E.M. *Fluid Mechanics*; Pergamon Press: Oxford, 1984.
- 20 Danov, K.D.; Ivanov, I.B. Critical film thickness and coalescence in emulsions. In *Proceedings of the Second World Congress on Emulsion*, September 23-26, 1997, Bordeaux, France; EDS Editeur: Paris, 1997; Contribution # 2-3.154.
- 21 Denkov, N.D.; Petsev, D.N.; Danov, K.D. Interaction between deformable Brownian droplets. *Phys. Rev. Letters* **1993**, 71 (19), 3226-3229.
- 22 Petsev, D.N.; Denkov, N.D.; Kralchevsky, P.A. Flocculation of deformable emulsion droplets II. Interaction energy. *J. Colloid Interface Sci.* **1995**, 176, 201-213.
- 23 Edwards, D.A.; Brenner, H.; Wasan, D.T. *Interfacial Transport Processes and Rheology*; Butterworth-Heinemann: Boston, 1991.
- 24 Beshkov, V.N.; Radoev, B.P.; Ivanov, I.B. *Int. J. Multiphase Flow* **1978**, 4, 563.
- 25 Davis, R.H.; Schonberg, J.A.; Rallison, J.M. *Phys. Fluids* **1989**, A1, 77.
- 26 Ivanov, I.B.; Traykov, T.T. Hydrodynamics of thin liquid films. Rate of thinning of emulsion films from pure liquids. *Int. J. Multiphase Flow* **1976**, 2, 397-410.
- 27 Ivanov, I.B.; Kralchevsky, P.A. Stability of emulsions under equilibrium and dynamic conditions. *Colloids Surfaces A* **1997**, 128, 155-175.
- 28 Russel, W.B.; Saville, D.A.; Schowalter, W.R. *Colloidal Dispersions*; Cambridge University Press, Cambridge, UK, 1989.
- 29 Danov, K.D.; Kralchevsky, P.A.; Ivanov, I.B. Dynamic processes in surfactant- stabilized emulsions. In *Encyclopedic Handbook of Emulsion Technology*; Sjoblom, J., Ed.; Marcel Dekker: New York, 2001; Chapter 26, p. 621-659.
- 30 Nemeth, Zs.; Sedev, R.; Ivanova, R.; Kolarov, T.; Exerowa, D. Thinning of microscopic foam films formed from a mixture of Bovine Serum Albumin and Pluronic L62. *Colloids Surfaces A* **1999**, 149, 179-184.
- 31 Velev, O.D.; Danov, K.D.; Ivanov, I. B. Stability of emulsions under static and dynamic conditions. *J. Dispersion Sci. Technol.* **1997**, 18 (6&7), 625-645.
- 32 Danov, K.D.; Velev, O.D.; Ivanov, I.B.; Borwankar, R.P. Bancroft rule and hydrodynamic stability of thin films and emulsions. In *Proceedings of the First World Congress on Emulsion*, October 19-22, 1993, Paris, France; Volume 2, Contribution # 1.21.125.
- 33 Davies, J.T.; Rideal, E.K. *Interfacial phenomena*; Academic Press: New York, 1963.
- 34 Traykov, T.T.; Manev, E.D.; Ivanov, I.B. Hydrodynamics of thin liquid films. Experimental investigation of the effect of surfactants on the drainage of emulsion films. *Int. J. Multiphase Flow* **1977**, 3, 485-494.

- 35 Chakarova, S.K.; Dupeyrat, M.; Nakache, E.; Dushkin, C.D.; Ivanov, I.B. The role of the surfactant distribution on the life-time of drops in the system water/ nitroethane. *J. Surface Sci. Technol.* **1990**, *6* (3), 201-215.
- 36 Basheva, E.S.; Gurkov, T.D.; Ivanov, I.B.; Bantchev, G.B.; Campbell, B.; Borwankar, R.P. Size dependence of the stability of emulsion drops pressed against a large interface. *Langmuir* **1999**, *15* (20), 6764-6769.
- 37 Velev, O.D.; Gurkov, T.D.; Borwankar, R.P. Spontaneous cyclic dimpling in emulsion films due to surfactant mass transfer between the phases. *J. Colloid Interface Sci.* **1993**, *159*, 497-501.
- 38 Danov, K.D.; Gurkov, T.D.; Dimitrova, T.D.; Ivanov, I.B.; Smith, D. Hydrodynamic theory for spontaneously growing dimple in emulsion films with surfactant mass transfer. *J. Colloid Interface Sci.* **1997**, *188* (2), 313-324.
- 39 Velev, O.D.; Gurkov, T.D.; Ivanov, I.B.; Borwankar, R.P. Abnormal thickness and stability of nonequilibrium liquid films. *Phys. Rev. Letters* **1995**, *75* (2), 264-267.
- 40 Gurkov, T.D.; Danov, K.D.; Velev, O.D.; Ivanov, I.B.; Borwankar, R.P. Stability of liquid films in non-preequilibrated emulsions. In *Proceedings of the Second World Congress on Emulsion (CME97)*, September 23-26, 1997, Bordeaux, France; EDS Editeur: Paris, 1997; Volume 2, Contribution # 2-3.155.
- 41 Kabalnov, A.; Wennerstrom, H. Macroemulsion stability: the oriented wedge theory revisited. *Langmuir* **1996**, *12* (2), 276-292.
- 42 Nikolova, A.; Exerowa, D. Rupture of common black films. Experimental study. *Colloids Surfaces A* **1999**, *149*, 185-191.
- 43 Tadros, Th.F.; Vincent, B. Emulsion stability. In *Encyclopedia of Emulsion Technology*; Becher, Paul, Ed.; Marcel Dekker: New York, 1983; Chapter 3, p. 129-285.
- 44 Gillespie, T.; Rideal, E.K. The coalescence of drops at an oil-water interface. *Trans. Faraday Soc.* **1956**, *52*, 173-183.

## FIGURE CAPTIONS

Figure 1.

Stages of thinning of the gap between two fluid particles (emulsion drops, gas bubbles), immersed in a continuous liquid phase and pushed toward each other by an external force. The system has rotational symmetry. See the text for the cases (a)-(f).

Figure 2.

Fluid velocity distribution (the arrows) during thinning of a plane-parallel film sandwiched between two liquid phases. The system has rotational symmetry. (a) Tangentially immobile interfaces; (b) Fully mobile interfaces (no surfactant); (c) Partial mobility in the presence of adsorbed surfactant. The bulk and surface diffusion fluxes which attempt to restore the uniform surfactant distribution on  $S$  are indicated. They are characterised by the diffusivities  $D$ ,  $D_s$ , respectively.

Figure 3.

Stability of oil drops pressed by buoyancy against a large oil/water interface. Measured lifetime,  $\tau$  (the points), is plotted vs. droplet radius,  $R_d$ , in a system consisting of soybean oil and aqueous solution of  $4 \times 10^{-4}$  wt% Bovine Serum Albumin + 0.15 M NaCl (pH=6.4). The inset illustrates the case of large drops, which undergo significant deformation so that a thin aqueous film forms between them and the big homophase.

Figure 4.

Non-equilibrium effects in emulsion films, due to surfactant redistribution between the bulk phases. (a) Schematic representation of the spontaneous cyclic formation, growth, and outflow of dimples, when the surfactant is initially dissolved in the continuous (film) phase and diffuses toward the surrounding oil; (b) Interference picture, in reflected monochromatic light, of a film containing dimple. The latter just starts flowing out. Black and white fringes correspond to thicknesses in multiples of  $\lambda/(4n)$  ( $\lambda$ = the light wavelength,  $n$ = the refractive index of the aqueous phase). The system contains 3.23 wt% nonylphenol polyoxyethylene-40 and 0.1 M NaCl dissolved in water, and styrene as oil; (c) Aqueous film with a channel, formed between xylene phases, in an experiment with  $5 \times 10^{-4}$  M Tween 20 (polyoxyethylene-20 sorbitan monolaurate) initially dissolved in the oil. The water phase contains 0.1 M NaCl. The arrows show the direction of the hydrodynamic fluxes. The film diameter is 450  $\mu\text{m}$ .

Figure 5.

Measured lifetime of soybean oil droplets pressed by buoyancy against a large soybean oil/water interface. The system contains  $7 \times 10^{-3}$  wt%  $\beta$ -casein (without  $\text{Ca}^{2+}$ ), salt- 0.15 M NaCl, pH= 6.4. In this range the lifetime does not depend on the drop size.

Figure 6.

Stability of oil drops pressed by buoyancy against an oil/water interface. The number of drops,  $N$ , which survive until the moment  $t$  (in an ensemble of  $N_{\text{tot}}$  drops) is plotted as a function of time.  $t_0$  denotes the moment when coalescence is first observed.

(a) Our measurements in a system containing  $7 \times 10^{-3}$  wt%  $\beta$ -casein (without  $\text{Ca}^{2+}$ ), large drops (1-3 mm), salt- 0.15 M NaCl, pH= 6.4, soya bean oil/water interface;  $-\log(N / N_{\text{tot}}) = 0.01250*(t-t_0) + 0.000240*(t-t_0)^2$ .

(b) Data of Gillespie & Rideal [44] for water drops at a paraffin/water interface (without surfactant); drop radius = 0.19 cm,  $T= 55^\circ\text{C}$ ;  $-\log(N / N_{\text{tot}}) = 0.0240*(t-t_0) + 0.001420*(t-t_0)^2$ .

(c) Our measurements in a system containing  $4 \times 10^{-4}$  wt% Bovine Serum Albumin (fatty acid free), salt- 0.15 M NaCl, pH= 6.5, soya bean oil/water interface;  $-\log(N / N_{\text{tot}}) = 0.09170*(t-t_0)$ .

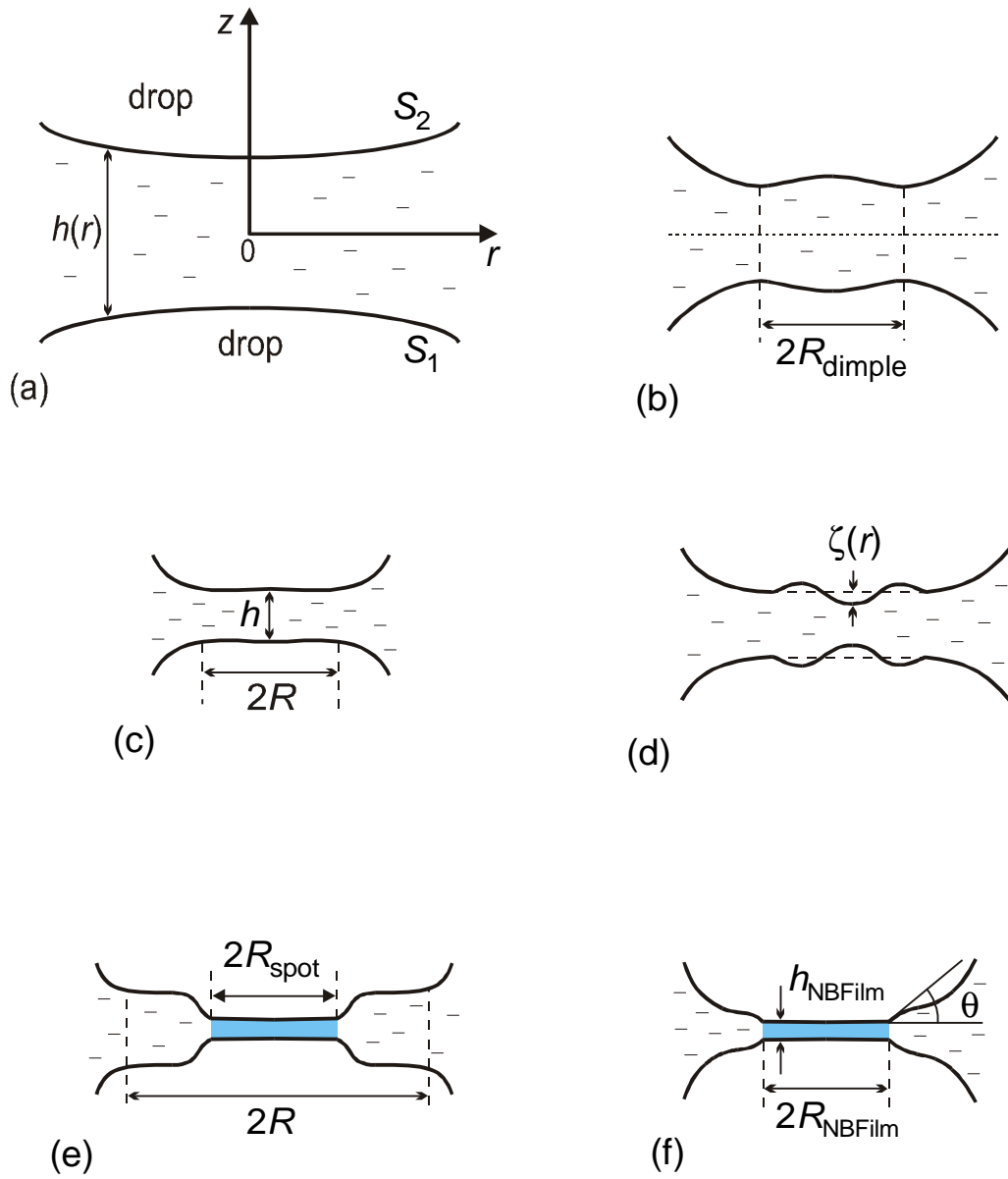


Figure 1.  
T. D. Gurkov *et al.*, "Hydrodynamic Behaviour and Stability of Approaching Deformable Drops"

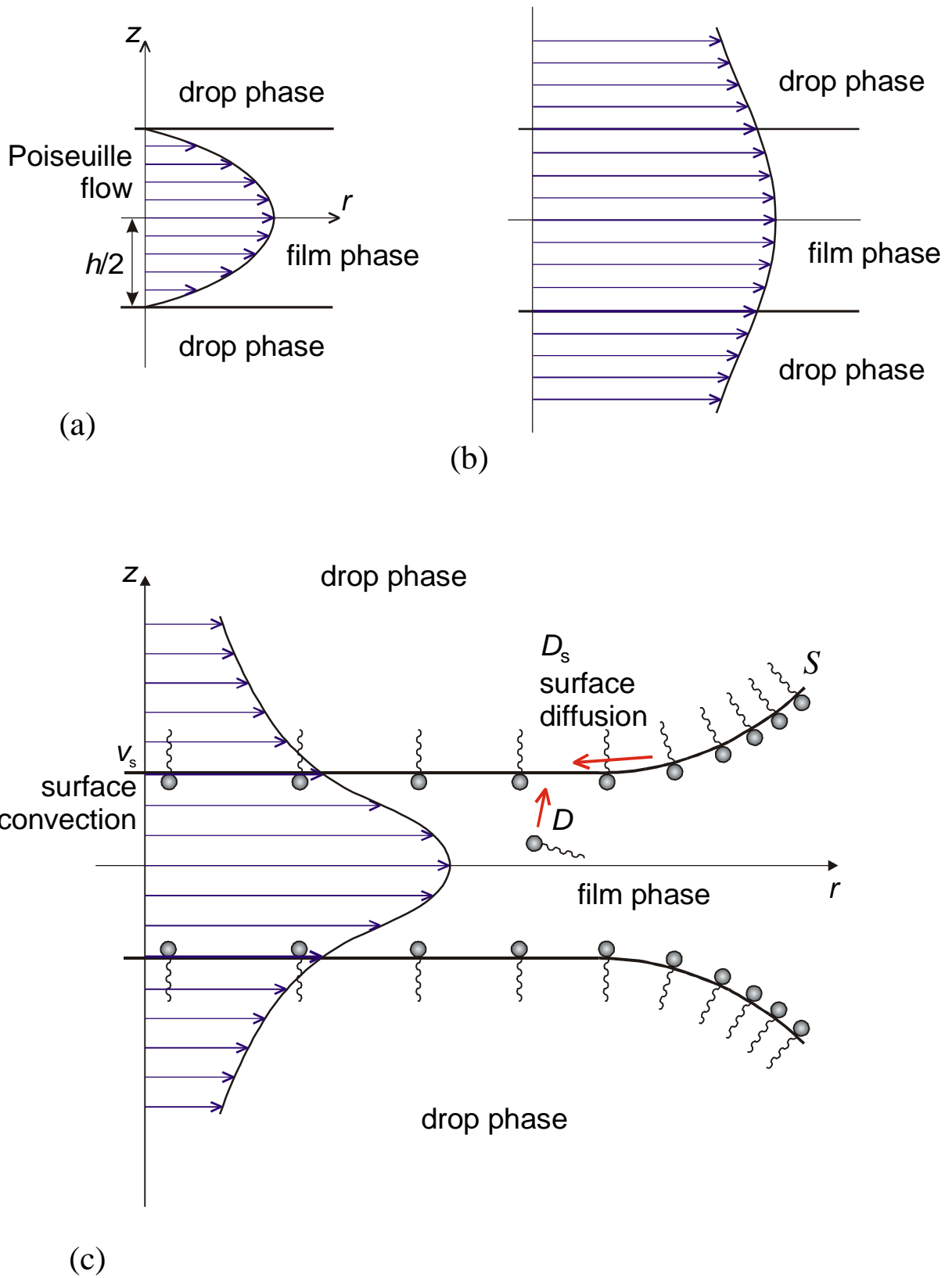


Figure 2.  
T. D. Gurkov *et al.*, "Hydrodynamic Behaviour and Stability of Approaching Deformable Drops"

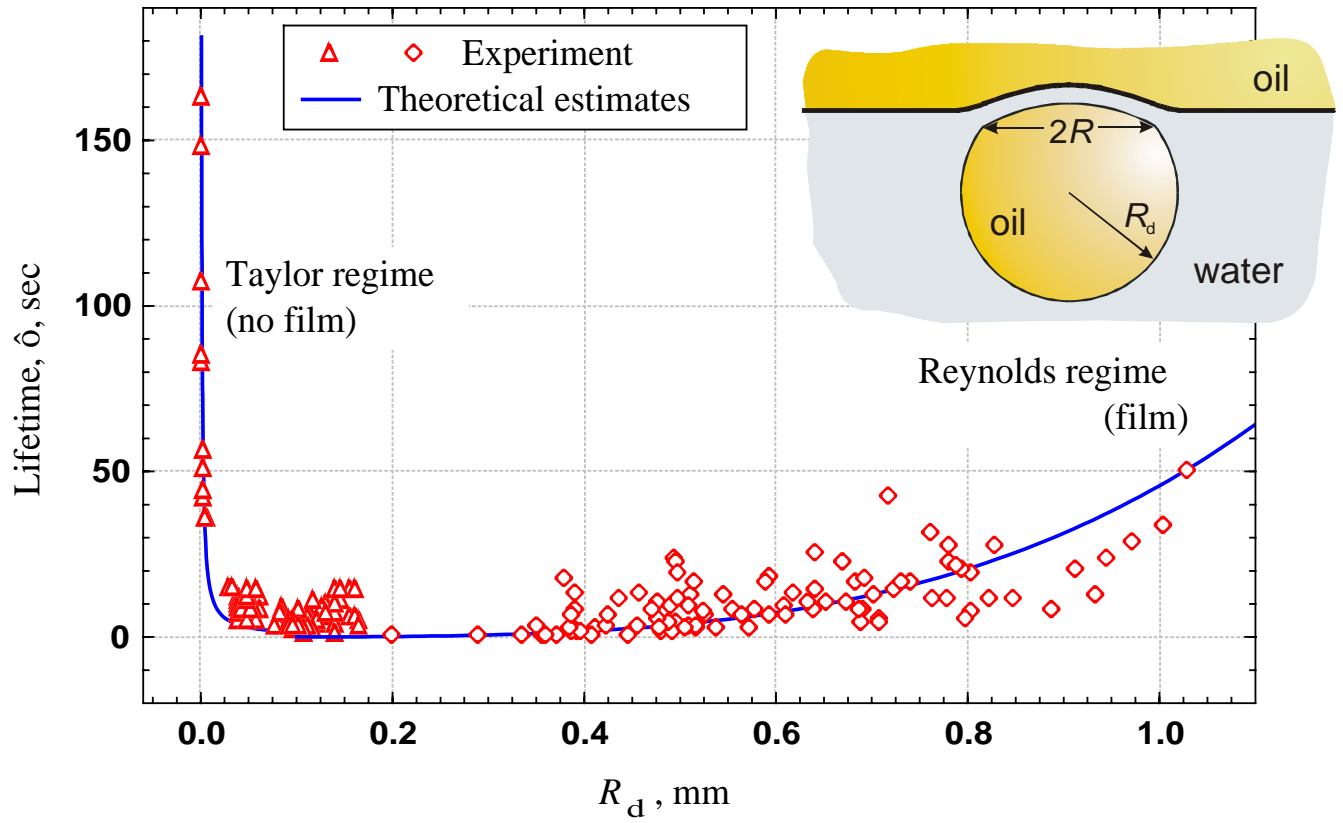


Figure 3.

T. D. Gurkov *et al.*, "Hydrodynamic Behaviour and Stability of Approaching Deformable Drops"

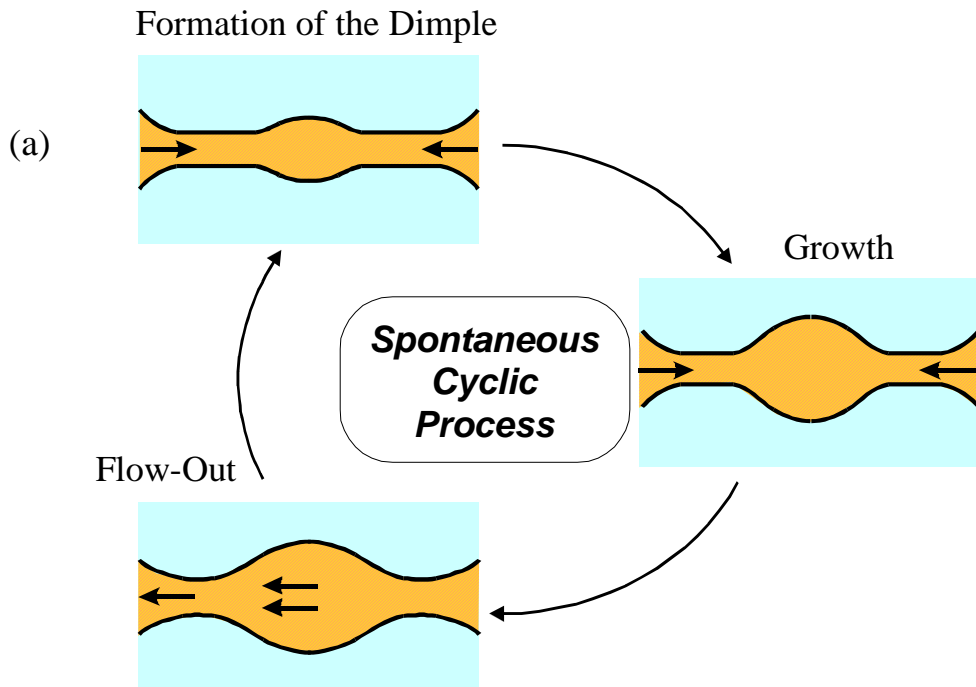


Figure 4 (a).

T. D. Gurkov *et al.*, “Hydrodynamic Behaviour and Stability of Approaching Deformable Drops”

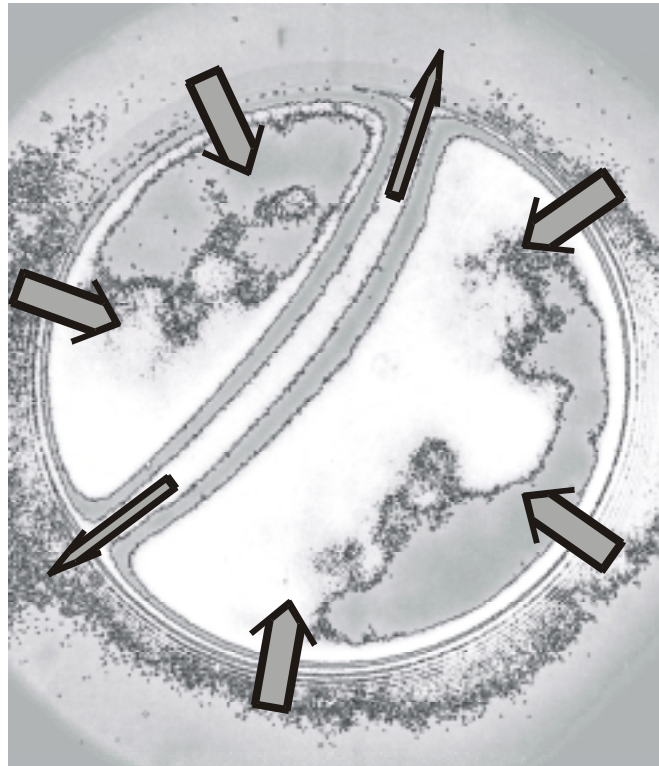
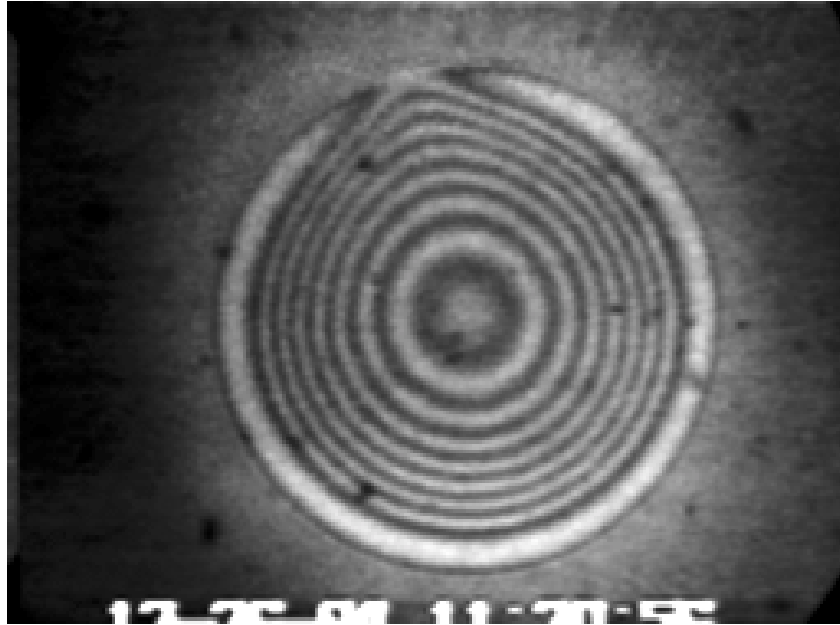


Figure 4 (b) and (c).

T. D. Gurkov *et al.*, "Hydrodynamic Behaviour and Stability of Approaching Deformable Drops"

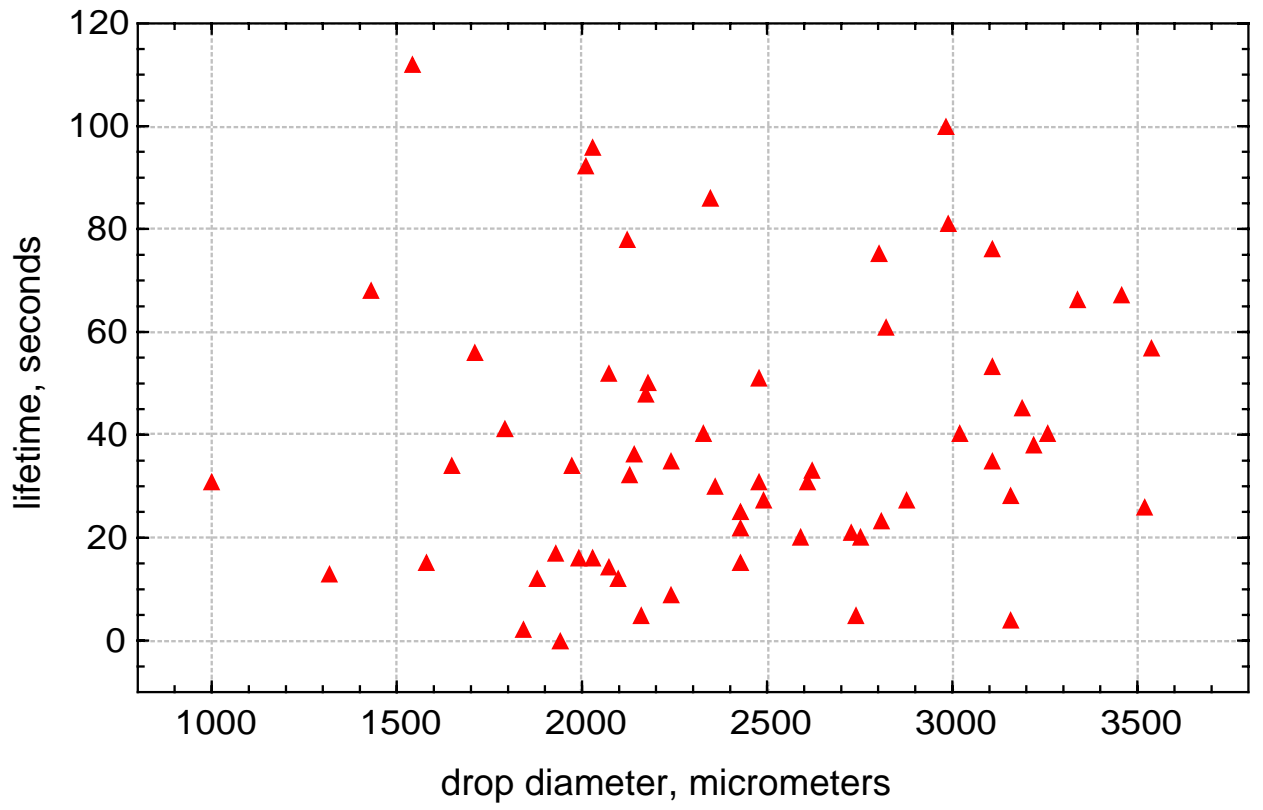


Figure 5.

T. D. Gurkov *et al.*, “Hydrodynamic Behaviour and Stability of Approaching Deformable Drops”

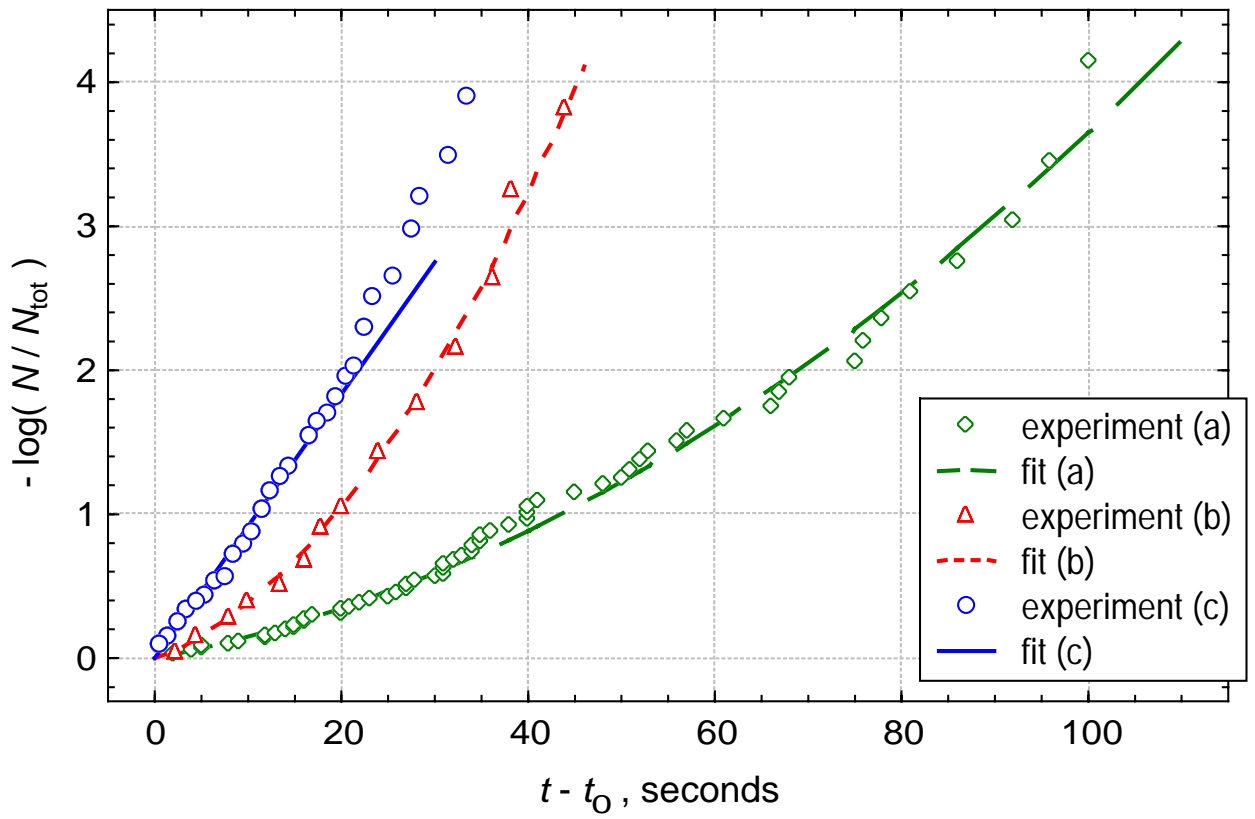


Figure 6.

T. D. Gurkov *et al.*, “Hydrodynamic Behaviour and Stability of Approaching Deformable Drops”